



## Research paper

# The role of connectivity and stochastic osteocyte behavior in the distribution of perilyabyrinthine bone degeneration. A Monte Carlo based simulation study



Sune Land Bloch\*, Mads Sølvsten Sørensen

Department of Otolaryngology Head and Neck Surgery and Audiology, Rigshospitalet, University of Copenhagen, Denmark

## ARTICLE INFO

## Article history:

Received 12 August 2015  
 Received in revised form  
 2 February 2016  
 Accepted 6 February 2016  
 Available online 10 February 2016

## Keywords:

Mathematical biology  
 Stochastic network model  
 Stochastic process  
 Deterministic process  
 Probability distribution  
 Connectivity  
 Monte Carlo method

## ABSTRACT

Previous studies of undecalcified temporal bones labeled with fluorescent tissue time markers and basic fuchsin have documented the unique spatial and temporal patterns underlying inner ear bone development, morphology and degeneration, and has led to the identification of inner ear OPG as the candidate inhibitor of perilyabyrinthine bone resorption. Resulting age related excessive matrix micro-damage, osteocyte death and degeneration of the OPG signaling pathway is expected to trigger bone remodeling in the otic capsule, but when this happens the morphology of the remodeling bone is abnormal and the distribution is not entirely smooth and predictable, but rather multifocal and chaotic with a centripetal predilection at the window regions, as in otosclerosis.

Based on the observed histological patterns, the fundamental preconditions of perilyabyrinthine bone cell behavior can be deduced. When this information is used to generate a virtual computer representation of the cellular signaling network, the fate of the aging network can be studied by 'virtual histology' in any number of simulated 'individuals'.

We demonstrate how a combination of simple osteocyte survival functions derived from histological observations and the effect of connectivity may account for gradual centripetal degeneration as well as occasional focal degeneration of the cellular anti resorptive signaling pathway around the fluid space of the inner ear and create a permissive environment for otosclerosis.

© 2016 Elsevier B.V. All rights reserved.

## 1. Introduction

Systematic studies of undecalcified mammalian temporal bones time labeled with bone seeking fluorochromes have documented that bone remodeling is highly inhibited around the inner ear space (Frisch et al., 2000). These findings predicted the existence of anti-resorptive signals originating from the inner ear space. The candidate inhibitor of perilyabyrinthine bone remodeling is the cytokine osteoprotegerin (OPG), which has been detected in high levels within the spiral ligament and fluid-filled inner ear space (Zehnder et al., 2005; Nielsen et al., 2014). The OPG signal may reach the otic capsular osteocytes by diffusion via the extracellular lacuno-canalicular porosity or by a cellular signal introduced via OPG to

the inner ear lining cells and subsequently propagated via the gap junctions of the osteocyte syncytium (Zehnder et al., 2005; Sørensen et al., 2005; Bloch and Sørensen, 2010a).

Because perilyabyrinthine bone turnover is low, the osteocytes and mineralized bone matrix are not replenished at the normal rate. Consequently, degeneration is expected to increase and, indeed, with age dead osteocytes do accumulate excessively in the perilyabyrinthine bone (Bloch and Sørensen, 2010a). Eventually, this degeneration may gradually disconnect the signaling network and interfere with the distribution of anti-resorptive signals (Sørensen et al., 2005; Bloch, 2012). Missing OPG signals may be important in the pathogenesis of otosclerosis since OPG knockout mice develop abnormal bone remodeling, stapes fixation and progressive loss of hearing (Kanzaki et al., 2006; Zehnder et al., 2006) and in human footplates a low expression of OPG has been measured in active otosclerosis by the use of OPG-specific RT-PCR (Karosi et al., 2011).

In the human otic capsule bone remodeling remains highly inhibited throughout life. However, in 3–5% of the population a

\* Corresponding author. Department of Otolaryngology Head & Neck Surgery and Audiology, Rigshospitalet, University of Copenhagen, Blegdamsvej 9, DK-2100 Copenhagen, Denmark.

E-mail address: [suneloch@hotmail.com](mailto:suneloch@hotmail.com) (S.L. Bloch).

significant increase of bone remodeling may present as otosclerosis, in which the morphology of the remodeling bone is abnormal and the distribution is not entirely smooth and predictable, but rather multifocal and chaotic with a centripetal predilection at the window regions (Bloch and Sørensen, 2010a). It is unknown at present what causes this irregular remodeling.

The dynamic patterns and the anti-resorptive inner ear signaling system were discovered by pooling and averaging the observations of centrifugal bone remodeling units, centripetal matrix microdamage, and dead osteocytes respectively from many histological sections to overcome the effect of stochastic variation in the relatively rare observations (Bloch and Sørensen, 2010a; Bloch, 2012; Frisch et al., 2015, 2000). This morphometric method was designed to identify smooth histological patterns but it is not well suited to describe and quantify such irregularities as found in capsular degeneration and otosclerotic remodeling.

Based on extensive studies of bulk-stained human temporal bones the spatial density gradients of viable and dead osteocytes have been determined at different ages (Bloch and Sørensen, 2010a; Bloch et al., 2012).

In the present study this information is used to generate a virtual computer representation of a simplified otic capsular signaling network, in which the fate of the aging network and the multicellular patterns, smooth as well as irregular can be studied by 'virtual histology' in any number of simulated 'individuals'.

A graphic account of the basics of perilyabyrinthine bone behavior and the present model system is presented in Fig. 1.

## 2. Materials and methods

### 2.1. The Monte Carlo method and some fundamental preconditions

In order to construct a virtual model of the labyrinthine osteocyte network, a suitable simulation method must be selected. The Monte Carlo method relies on repeated random sampling (*iterative calculations*) to evaluate a deterministic model when the input of the model depends on uncertain parameters. The method is highly appropriate when the model is complex and nonlinear and involves several uncertain parameters. Simulation of biological systems relies on data from "real" observations and assumptions based on knowledge of the system studied. Individual osteocyte life length varies, while the average osteocyte life length depends on the distance to the inner ear space. Consequently, the fate of any osteocyte can be modeled as a game of life or death by lottery to reflect aging, and ruled by an odds function with a higher death risk near the inner ear to reflect the observed distribution. In addition, any osteocyte must die when connectivity is lost by the death of neighboring cells. The compound model must produce an average distribution of dead osteocytes identical to the one observed in bulk-stained human temporal bones.

### 2.2. Building a simplified network model of labyrinthine osteocytes

Osteocytes are connected to each other by a complex branching network of cell processes located within the lacuno-canalicular porosity. The number of cell processes emanating from an osteocyte and the connections between adjacent osteocytes are variable and high (Remaggi et al., 1998; Sugawara et al., 2011). However, in this model, the nearest neighboring osteocytes were connected to each other by a single pathway within a cubic lattice network with the dimensions of  $10 \times 10 \times 10$  nodes (Microsoft Excel 2007). This is the simplest way to model how the communication between two adjacent cells is lost when an osteocyte dies, despite lacking information of the exact number of inter-cellular connections. This simplification relies on the fact that the patency of the lacuno-

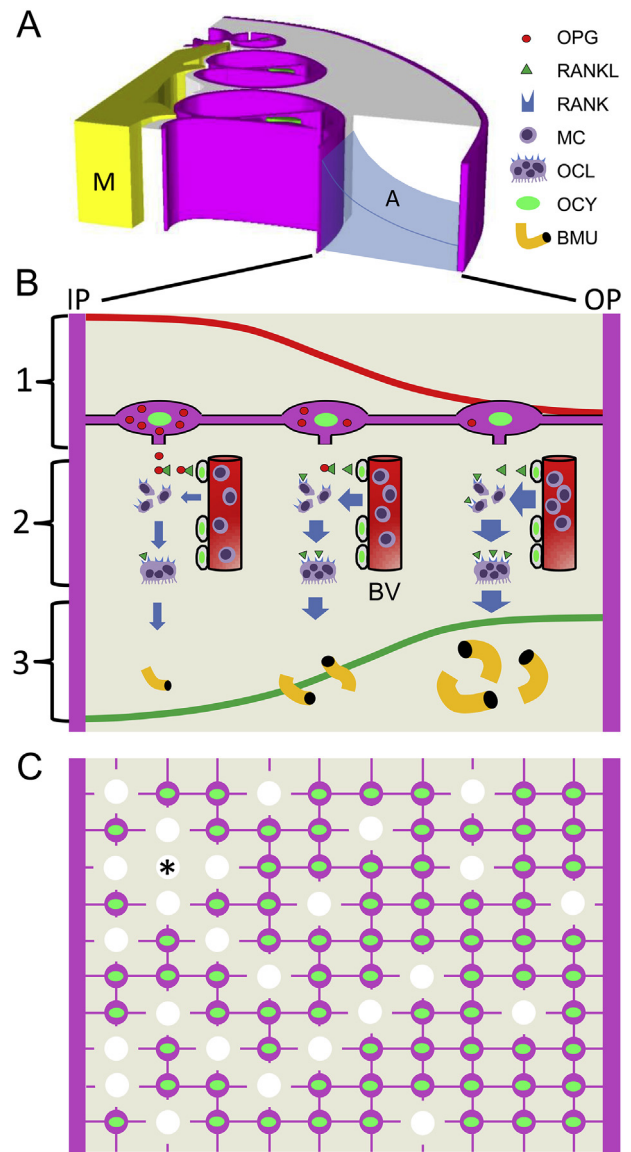


**Fig. 1.** Schematic presentation of a possible basic physiological mechanism of bone cell dynamics in the otic capsule. Panel A. A boxed volume of a full thickness of bony otic capsule. Transparent plot A illustrates how the inhibition of bone remodeling is distributed centripetally around the inner ear space. Modiolus = yellow, inner (IP) and outer (OP) periosteal bony layer = pink, capsular bone = light gray. Panel B. A view into the box. Level 1 shows a red plot of the concentration gradient of anti-resorptive OPG diffusing through the peri-osteocytic lacuno-canalicular porosity from the inner ear towards the capsular periphery. Level 2 shows how inner ear OPG and osteocytic RANKL compete for the RANK receptor of circulating monocytes to inhibit, or stimulate local osteoclast formation and resorptive activity. At the inner periost OPG inhibition is dominating, while towards the periphery the balance shifts in favor of RANKL stimulation. Level 3 illustrates the resulting lack of BMU based osteonal remodeling in perilyabyrinthine bone, and the gradual increase towards normal systemic remodeling activity at the capsular periphery, green plot. Panel C. The final tissue level effect of insufficient osteocyte replenishment caused by prolonged perilyabyrinthine inhibition of bone remodeling is excessive osteocyte death, centripetally distributed on average, with a higher rate of cell death closer to the inner ear spaces. For virtual simulation of further details of distribution and variance of capsular osteocyte death a cellular 3-D lattice network model as illustrated here in 2-D was built. Viable cells were removed by a probabilistic function modeled on observed histological data, and by the death of neighboring cells (note asterisk on disconnected center cell in a perilyabyrinthine void). OPG, osteoprotegerin; RANKL, receptor activator of nuclear factor-kappa  $\beta$  ligand; RANK, receptor activator of nuclear factor-kappa  $\beta$ ; MC, monocyte; OCL, osteoclast; OCY, viable osteocyte; BMU, basic multicellular unit; BV, blood vessel.

canalicular porosity is eventually lost around an empty lacuna (dead osteocyte) when the vital trimming action of the osteocyte matrix metalloproteinases seizes (Holmbeck et al., 2005; Inoue et al., 2006).

### 2.3. Simulating the degeneration of labyrinthine osteocytes based on histological data

In the first step and the stochastic part of the model, the passage of time in a specific individual was simulated. The fate (alive or dead) of each osteocyte of the network was determined at random by a probabilistic cell-survival function (input distribution) based on data from a sub-sample of previous histological observations and the use of pseudo random numbers. The sub-sample corresponded to the average spatial density gradients of viable and dead osteocytes across the cochlear wall in aging undecalcified human temporal bones bulk-stained with basic fuchsin (mean = 83 y, range 73–95 y,  $n = 20$ ). In this sample (Fig. 2), the average fraction of dead osteocytes was approximately 50% adjacent to the inner ear space, with a gradual nonlinear decline to 15% at the capsular periphery (Bloch and Sørensen, 2010a). The probabilistic cell-survival function was validated in numerous simulations and produced average spatial input distributions of dead and viable osteocytes across the cochlear wall (Fig. 2) identical to the one observed in bulk-stained human specimens (Bloch and Sørensen, 2010a). The connections to the osteocytes facing the lining cells of the inner ear space and the outer periost were *a priori* given positive inputs since these soft tissue compartments were always considered viable *in vivo*. The input to the border osteocytes of the remaining network (top, bottom and the two sides of the model) was, as the rest of the network, depending on the histologically derived stochastic cell-survival function. Hence, the degree of freedom of the model was  $1000 + 4 \times 100 = 1400$ . Only data from the 1000 node cubic lattice was analyzed and displayed.

### 2.4. Simulating the effect of connectivity on the degeneration of the labyrinthine osteocytes

In the second step and deterministic part of the model the fate of the remaining osteocyte survivors was then further adjusted to comply with the state of connectivity to their nearest neighboring osteocytes in the x, y and z plane. Because osteocytes must exchange metabolites with the general circulation to exist within the mineralized bone matrix, the patency of the lacuno-canalicular conduit is crucial for the survival of individual osteocytes (Benou et al., 2006). Therefore, the physical condition of individual osteocytes may be fatal below a critical number of connections to the adjacent osteocyte network. Currently, the exact number of connections needed for the survival of an osteocyte remains unknown. Therefore, the critical threshold of osteocyte survival defined by the degree of connectivity to the nearest neighboring osteocytes was simulated at different thresholds. The osteocyte survivors were automatically removed if the nearest neighbor population of viable osteocytes was less than or equal to 17%, 33% or 50% (1, 2 or 3 out of 6). These conditions explored the effect of variable degrees of further osteocyte death within the network until a steady state was reached (the number of re-calculations in step 2 was set to 1000 due to the size of the model).

### 2.5. Simulating the combined effect of aging and connectivity on the labyrinthine osteocytes

By initializing step 1 (stochastic part) followed by step 2 (deterministic part) the combined effect of aging and connectivity was simulated corresponding to one life history, i.e. one iteration.

Finally, the inter-individual variation was studied by repeating the compound simulation in series of 50 iterations to study the virtual life histories of 50 temporal bones. Average output distributions for the different parameter estimates were obtained for the 3 different settings of connectivity thresholds (Fig. 2). A steady state for the simulated average values of the different parameter estimates was typically approximated already after 20 iterations.

### 2.6. From algebra to three-dimensional presentation of data

The transformation of mathematical algorithms into a 3D display required several steps. First, the output distributions of each iteration of the Monte Carlo simulation were displayed in 2D by series of  $10 \times 10$  cells and the fate of each osteocyte highlighted as “o” to signify an osteocyte dead by aging, “x” to signify a viable osteocyte and “ $\times$ ” to signify an osteocyte dead by disconnection. Data were automatically imported into Photoshop (Version 12.0, © 2010, Adobe Systems Incorporated) as image files by using a macro. By the use of the “actions” routine to perform automated tasks, the image series was then transformed into a more representative visual display by creating a well-defined boundary around the osteocyte symbols and, as a central step, different gray tones added to the 3 different viability states of the osteocytes. In the third step, the processed images were imported into the open-source software Reconstruct (<http://synapses.clm.utexas.edu/tools/reconstruct/reconstruct.stm>). By using the “Wildfire Region Growing” routine combined with different settings of gray tone thresholds (made possible only by the preceding step in Photoshop), automated delineation of the boundary profiles of the osteocytes symbols was performed. Finally, different colors were added to highlight dead, viable and disconnected osteocytes.

## 3. Result

### 3.1. Preliminary analysis based on unadjusted probabilistic cell-survival functions

The initial Monte Carlo simulations generated average output distributions of dead osteocytes  $\sum$  dead by aging + disconnection, which were notably higher than the observed and the histology-derived probabilistic cell-survival functions (Fig. 2). The degree of oversampling was highly correlated to the applied connectivity-thresholds (Fig. 2A–C, column 1). For instance, when a low threshold of osteocyte survival was applied, i.e. an osteocyte must die if the survival of the nearest neighbor osteocytes was equal to or less than 50%, the entire remaining network of osteocyte survivors was subsequently disconnected in every iteration (Fig. 2A, column 1). The effect of overestimation was notably smaller when a high threshold of osteocyte survival by the connectivity factor was applied (Fig. 2C, column 1).

### 3.2. Model predicted effect of connectivity based on adjusted probabilistic cell-survival functions

In order to eliminate the overestimation of dead osteocytes and produce output distributions that approximated the histological data, different probabilistic cell-survival functions were tested in thousands of iterations until functions were found for which the average output distributions of dead osteocytes across the simulated box volume did eventually match the histological data for the 3 different threshold settings of connectivity (Fig. 2A–C, column 2). Repeated random sampling based on the adjusted input variables demonstrated how the risk (amount) of osteocyte death by disconnection was generally higher towards the inner ear space compared to the capsular periphery of the otic capsule (Fig. 2A–C,

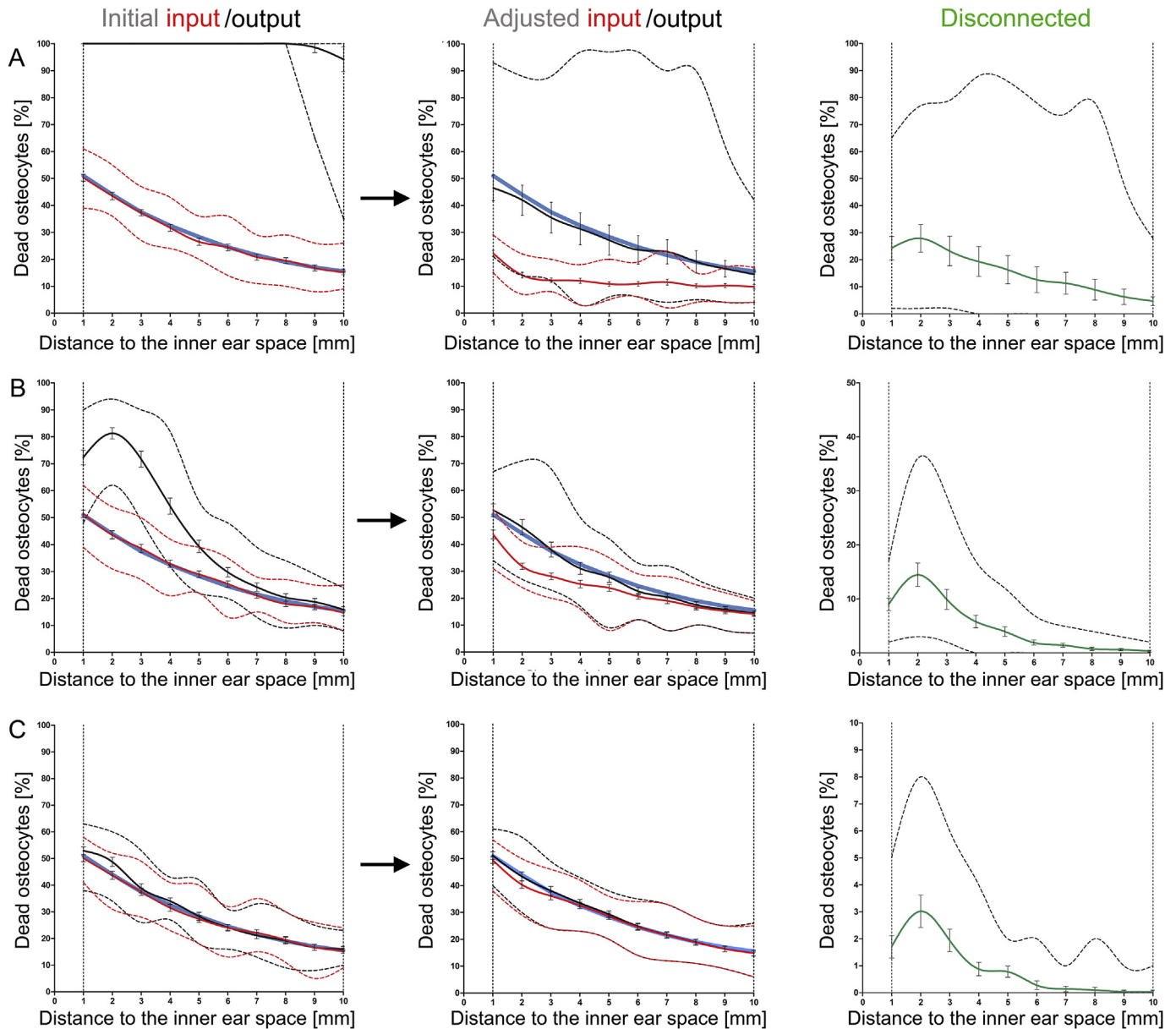


**Fig. 2.** The modeling of a compound stochastic/deterministic model of perilyabyrinthine osteocyte death. The blue plot shows the average distribution of dead osteocytes around the inner ear space as measured by histomorphometry in 20 older human temporal bones bulk stained with basic fuchsin. The red plots A, B and C in the first column show the distribution of dead osteocytes in a virtual box of perilyabyrinthine bone as calculated by an input probability function of osteocyte death modeled on the measured histological distribution. The black plots in the first column show the distributions of dead osteocytes as calculated by the probability function in combination with an additional deterministic death-by-disconnection routine with a variable connectivity cut-off point of A:50%, B:33% or C:17%, each plot is averaged from 50 iterations. The simulated output distributions are “overshooting” at A and B and to a lesser extent in C because the stochastic death rate of the probability function initially selected was set too high given the additional effect of osteocyte death as the result of disconnection. The second column shows how a new adjusted probability function (red lines) can take account of the added disconnection routine to approximate the compound output simulation data to the histological observations. The third column with varied scales on the y axis highlights the amount and distribution of osteocytes dead by disconnection at the 3 different cut-off settings. Error bars indicate 95% CI and the dashed lines min/max values for the different parameter estimates of the 50 iterations.

column 3). The average proportion of disconnected osteocytes was high when the viability of the individual osteocyte was allocated to be sensitive to the death of the nearest neighboring osteocytes, i.e. applying a low connectivity-threshold of osteocyte survival (Fig. 2A, column 3). Correspondingly, the proportion of disconnected cells was low when a high connectivity-threshold of osteocyte survival was applied (Fig. 2C, column 3), i.e. the network became more robust to the stochastic variations of osteocyte death.

### 3.3. Visual interpretation

Three-dimensional reconstructions were added to selected series of the Monte Carlo simulation by using the intermediate connectivity factor of 33%, i.e. osteocyte survivors must die if the nearest neighbor population of viable osteocytes is equal to or less than 33%. The use of visual displays added important information of cellular spatial distribution and irregularities that could never be deduced from the analysis of 2D data alone (Fig. 3A). The visual outputs were never the same, since the combination of possible

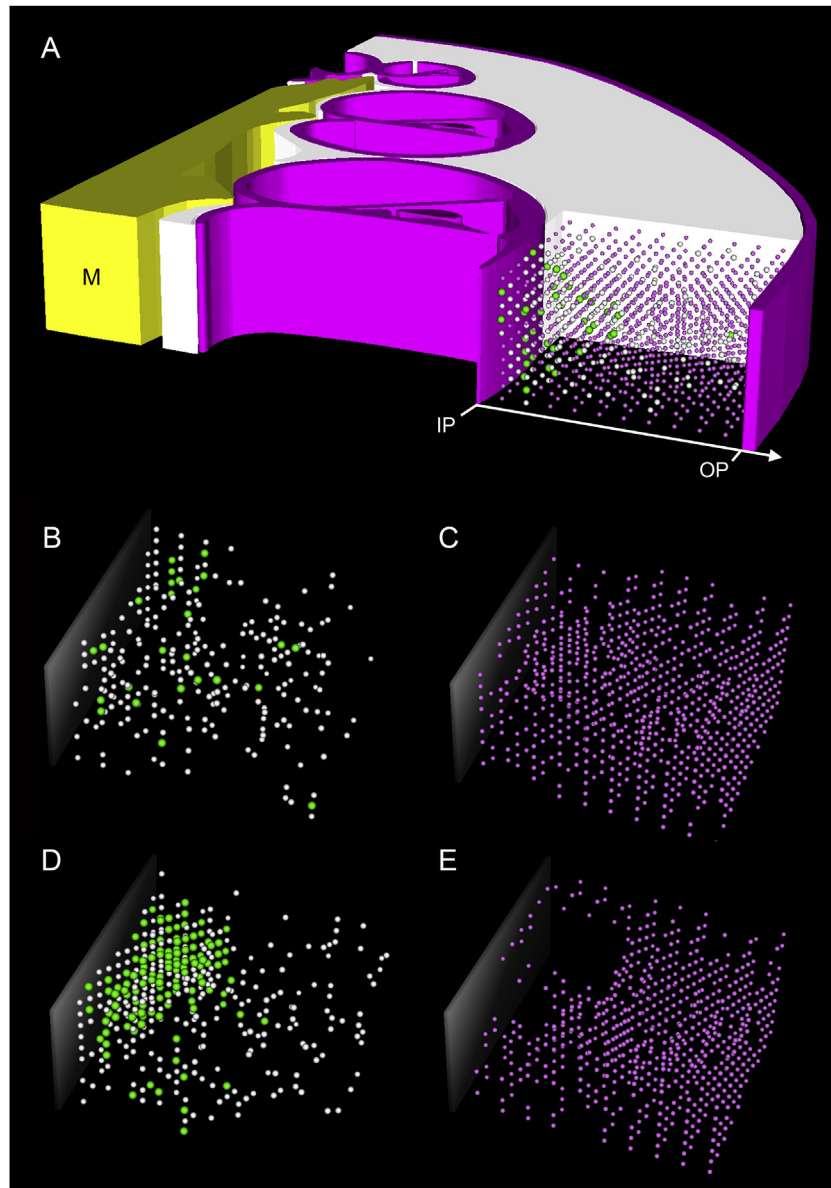


**Fig. 3.** Three-dimensional virtual box model of 1000 perilyabyrinthine osteocytes all interconnected within a network (interconnections are not displayed) facing the inner periosteal layer at IP and the outer periosteal layer at OP (A). The fate of each individual osteocyte was simulated repeatedly by random sampling based on adjusted probabilistic cell-survival functions in order to comply with histological data. In most iterations, dead osteocytes were forming a smooth centripetal distribution around the inner ear spaces (B), while the viable osteocytes showed a smooth centrifugal distribution (C). In some of the iterations, irregular clustering of dead osteocytes with a preference near the inner ear space was identified (D). Osteocytes dead by disconnection contributed highly to these cellular voids, which were surrounded by an intact and viable osteocyte network (E). M, Modiolus; White dots, osteocytes dead by stochastic variations; Green dots, osteocytes dead by disconnection; Purple dots, viable osteocytes.

inputs into the model before each iteration was extreme and given by 21,000, i.e. 1000 cells, each with two possible values, viable or dead (Fig. 4).

In most of the iterations dead osteocytes were centripetally and relatively smoothly distributed across the capsular wall (Fig. 3B) while the osteocyte survivors were centrifugally distributed (Fig. 3C). However, in some iterations, clustering of dead osteocytes was observed with a spatial preference near the inner ear space (Fig. 3D). In most of these iterations, the shape and size of the clusters were globular and very small (Fig. 4; I1B, I4B, I5B). However, in some iterations larger clusters of dead osteocytes were identified (Fig. 3D). Moreover, these regions were surrounded by an intact network of viable osteocytes (Fig. 3E). The occasional cellular

voids were composed partly of dead osteocytes clustering at random merely by stochastic variation, and partly of additional disconnected osteocytes, which was frequently the dominant cell type (Fig. 3D). In the large clusters the shape of the void appeared to be anisotropic with the largest volume facing the inner ear space (Fig. 3D–E).

#### 4. Discussion

This study demonstrates how a combination of simple osteocyte survival functions and the effect of connectivity may account for gradual as well as focal degeneration of the cellular network within the otic capsule. The Monte Carlo method is highly appropriate to

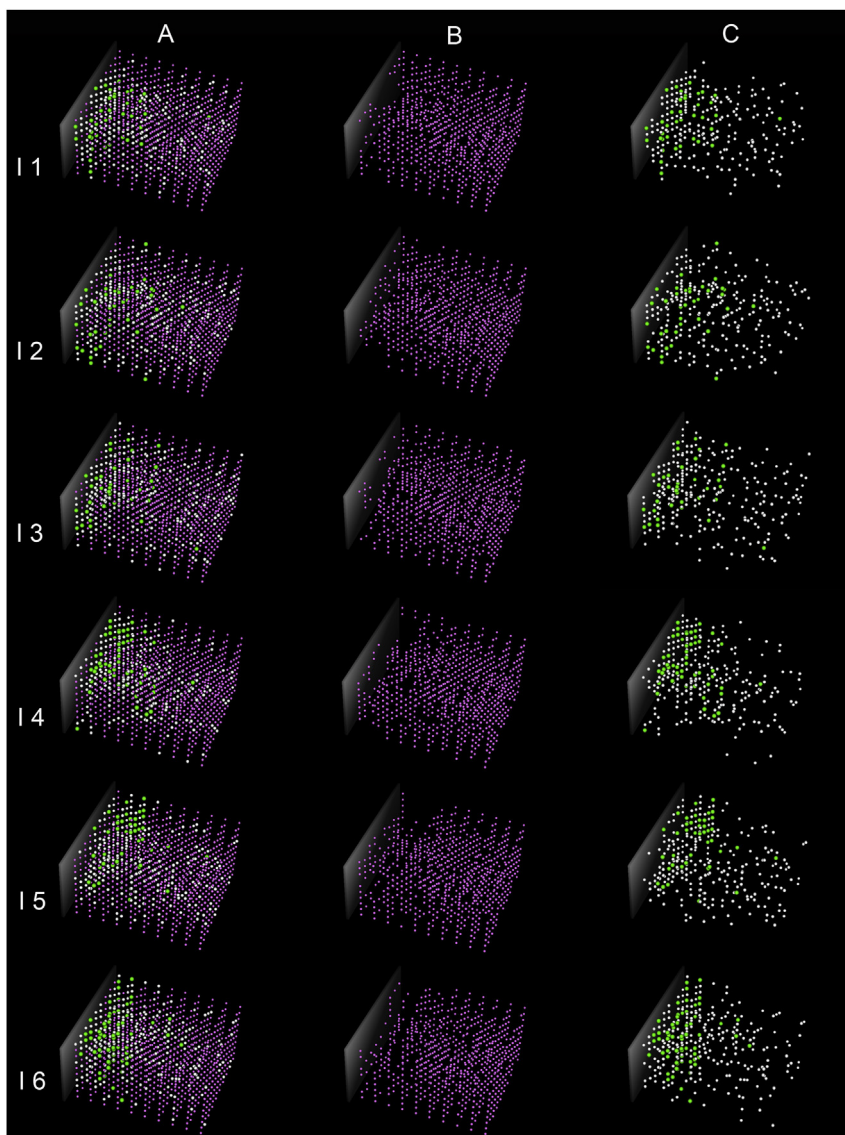


**Fig. 4.** Visual outputs of another six random iterations of the same simulation routine illustrating how details of the spatial distribution of cellular degeneration may vary as a result of stochastic cell behavior and the effect of death by disconnection. Column A shows the total population of viable osteocytes (purple dots), osteocytes dead by stochastic aging (white dots) and osteocytes dead by disconnection (green dots) for the iterations I1–I6. Column B depicts only the viable part of the osteocyte network, and column C highlights the dead part of the degenerating osteocyte network.

evaluate a deterministic model of the osteocyte network because the input of the model depends on uncertain parameters, a task which in the past was only possible by the use of supercomputers.

Under normal conditions bone remodeling is highly suppressed around the inner ear space of the otic capsule (Frisch et al., 2000). The candidate inhibitor of perilyabyrinthine bone remodeling is the cytokine OPG, which is highly expressed within the soft matrix of the inner ear space (Zehnder et al., 2005), but other mechanisms may be involved in the maintenance of the anti-resorptive environment of the otic capsule (Stankovic et al., 2010; Nielsen et al., 2014). The OPG-signal has been suggested to enter the surrounding otic capsule via the lacuno-canalicular porosity, which contains the viable network of labyrinthine osteocytes. With advancing age, dead osteocytes accumulate around the inner ear space because the average age of the bone matrix and the embedded osteocytes increases much faster than in remodeling bones in the rest of the skeleton (Bloch and Sørensen, 2010a; Bloch et al., 2012). The spatial pattern of the degenerating osteocyte network has been

extensively studied by the use of bulk-stained human temporal bones (Bloch and Sørensen, 2010a). Death of an osteocyte is followed by occlusion of its local lacuno-canalicular environment, which may gradually impede the network and eventually prevent the distribution of OPG signals through the bone. However, the fetal density of labyrinthine osteocytes is extremely high and may therefore sustain a life-long pathway for anti-resorptive signals as long as the accumulation of dead osteocytes is smoothly distributed (Bloch and Sørensen, 2010a). It is noteworthy that in a healthy subject the density of viable labyrinthine osteocytes is equal to that of age-matched bone samples from ribs even in old age, although the density of dead osteocytes is much higher in the temporal bone (Bloch et al., 2012).

In most of the output iterations of the simulated osteocyte network, the accumulation of dead osteocytes was centripetally and smoothly distributed. In this case, an anti-resorptive signaling field may well persist around the inner ear space in aging subjects although the connectivity of the signaling pathway is less

compared to young individuals. However, occasional clustering of dead osteocytes may locally impede the effect of anti-resorptive signals leaving the void regions unprotected against focal bone remodeling. Since the surrounding signaling network is otherwise intact it may still influence and distort the morphology of the focal bone remodeling, as in human otosclerosis. We have previously reported the occasional clustering of dead osteocytes in perilymphatic bone bulk-stained with basic fuchsin (Sørensen et al., 2005; Bloch and Sørensen, 2010a; Bloch et al., 2012; Bloch, 2012). Moreover, we have demonstrated how the otosclerotic lesions are preferentially distributed towards the inner ear space of the otic capsule, with a smooth demarcation against the surrounding bone. Larger lesions have a bulky end facing the inner ear space (Bloch and Sørensen, 2012, 2010b). These anatomical observations share a remarkable similarity to the simulated focal degeneration of the osteocyte network by its sporadic occurrence, preferential location close to the inner ear space, focal and anisotropic shape of the lesions, and smooth demarcation against the surrounding, viable parts of the osteocyte network. The present findings provide a stochastic element to expand and consolidate the osteodynamic concept of the pathogenesis of otosclerosis, which may comment on a number of clinical characteristics of this disease. They present a mechanism, which may link bone degeneration to bone remodeling, and suggest, that the trigger of bone remodeling is not necessarily a signal that is turned on. It may be a signal that is turned off.

Simulation of biological systems relies, as far as possible, on data from real observations of the system studied. However, since most biological systems are highly complex, several parameters may be unknown or only partly elucidated. For this reason, a number of assumptions must be made in order to create a feasible model for the analysis of the behavior of the biological system under different circumstances. Stochastic network models have previously been used to study the molecular sieving characteristics of bone by connecting each of the nodes of the network model to its immediately neighboring six nodes (Steck and Tate, 2005). We used a similar approach. However, the *in vivo* connectivity of the osteocyte network is highly complex and a challenging task to map as demonstrated in animal studies based on LM (Remaggi et al., 1998), SEM (Schneider et al., 2011), 3D reconstruction (Sugawara et al., 2005) and unfolding mathematical algorithms (Beno et al., 2006). The number of cell processes emanating from an osteocyte and the connections between adjacent osteocytes appear to be high, variable and affected by age as well as disease (Power et al., 2002; Vashishth et al., 2000). Future stochastic network models of the labyrinthine osteocytes and porosity should be based on refined reconstructions of the osteocyte network based on detailed observations from bulk-stained human temporal bones. Moreover, the critical threshold of connectivity for osteocyte death should be determined by exploring the histological characteristics of bulk-stained human osteocytes combined with unfolding mathematical algorithms. The spatial pattern, frequency and size of perilymphatic focal bone degeneration as demonstrated histologically by the clusters of dead osteocytes should be further investigated in bulk stained materials, and reproduced in more refined virtual models, which may simulate the bone dynamics of the otic capsule. Additional models may include reconstructions of the entire otic capsule with a focus on the predilection sites of otosclerosis, the impact of microdamage and the addition of the vascular systems to further improve the realism of the computerized simulation.

## 5. Conclusion

The simulated degeneration of osteocytes in a virtual network model was generally smooth and centripetally distributed

mimicking the action of a histological pathway for anti-resorptive signals across the thickness of the otic capsule preserved even in aging subjects. However, occasional clustering of dead and disconnected osteocytes, as previously found in histological specimens, could form simply by stochastic variation in the virtual model to create signaling voids not protected against focal bone remodeling, and bring about a possible permissive environment for otosclerosis.

## Conflicts of interest

None.

## Financial conflict of interest

None.

## References

- Beno, T., Yoon, Y.J., Cowin, S.C., Fritton, S.P., 2006. Estimation of bone permeability using accurate microstructural measurements. *J. Biomech.* 39, 2378–2387.
- Bloch, S.L., 2012. On the biology of the bony otic capsule and the pathogenesis of otosclerosis. *Dan. Med. J.* 59, B4524.
- Bloch, S.L., Kristensen, S.L., Sørensen, M.S., 2012. The viability of perilymphatic osteocytes: a quantitative study using bulk-stained undecalcified human temporal bones. *Anat. Rec.* 295, 1101–1108.
- Bloch, S.L., Sørensen, M.S., 2012. Otosclerosis: a perilymphatic threshold phenomenon. *Acta Otolaryngol.* 132, 344–348.
- Bloch, S.L., Sørensen, M.S., 2010a. The viability and spatial distribution of osteocytes in the human labyrinthine capsule: a quantitative study using vector-based stereology. *Hear. Res.* 270, 65–70.
- Bloch, S.L., Sørensen, M.S., 2010b. Three-dimensional reconstruction of the otosclerotic focus. *Acta Otolaryngol.* 130, 429–434.
- Frisch, T., Bloch, S.L., Sørensen, M.S., 2015. Prevalence, size and distribution of microdamage in the human otic capsule. *Acta Otolaryngol.* 135, 771–775.
- Frisch, T., Overgaard, S., Sørensen, M.S., Bretlau, P., 2000. Estimation of volume referent bone turnover in the otic capsule after sequential point labeling. *Ann. Otol. Rhinol. Laryngol.* 109, 33–39.
- Holmbeck, K., Bianco, P., Pidoux, I., Inoue, S., Billingham, R.C., Wu, W., Chrysovergis, K., Yamada, S., Birkedal-Hansen, H., Poole, A.R., 2005. The metalloproteinase MT1-MMP is required for normal development and maintenance of osteocyte processes in bone. *J. Cell Sci.* 118, 147–156.
- Inoue, K., Mikuni-Takagaki, Y., Oikawa, K., Itoh, T., Inada, M., Noguchi, T., Park, J.-S., Onodera, T., Krane, S.M., Noda, M., Itoharu, S., 2006. A crucial role for matrix metalloproteinase 2 in osteocytic canalicular formation and bone metabolism. *J. Biol. Chem.* 281, 33814–33824.
- Kanzaki, S., Ito, M., Takada, Y., Ogawa, K., Matsuo, K., 2006. Resorption of auditory ossicles and hearing loss in mice lacking osteoprotegerin. *Bone* 39, 414–419.
- Karosi, T., Csomor, P., Szalmás, A., Kónya, J., Petkó, M., Sziklai, I., 2011. Osteoprotegerin expression and sensitivity in otosclerosis with different histological activity. *Eur. Arch. Oto-Rhino-Laryngol.* 268, 357–365.
- Nielsen, M.C., Martin-bertelsen, T., Friis, M., Winther, O., Friis-hansen, L., Rye-Jørgensen, N.R., Bloch, S., Mads, S.S.L., 2014. Differential gene expression in the otic capsule and the middle ear – an annotation of bone-related signaling genes. *Otol. Neurotol.* 36, 727–732.
- Power, J., Loveridge, N., Rushton, N., Parker, M., Reeve, J., 2002. Osteocyte density in aging subjects is enhanced in bone adjacent to remodeling haversian systems. *Bone* 30, 859–865.
- Remaggi, F., Canè, V., Palumbo, C., 1998. Histomorphometric study on the osteocyte lacuno-canalicular network in animals of different species. I. Woven-fibered and parallel-fibered bones. *Ital. J. Anat. Embryol.* 103, 145–155.
- Schneider, P., Meier, M., Wepf, R., Müller, R., 2011. Serial FIB/SEM imaging for quantitative 3D assessment of the osteocyte lacuno-canalicular network. *Bone* 49, 304–311.
- Stankovic, K.M., Adachi, O., Tsuji, K., Kristiansen, A.G., Adams, J.C., Rosen, V., McKenna, M.J., 2010. Differences in gene expression between the otic capsule and other bones. *Hear. Res.* 265, 83–89.
- Steck, R., Tate, M.L.K., 2005. In silico stochastic network models that emulate the molecular sieving characteristics of bone. *Ann. Biomed. Eng.* 33, 87–94. <http://dx.doi.org/10.1007/s10439-005-8966-7>.
- Sugawara, Y., Ando, R., Kamioka, H., Ishihara, Y., Honjo, T., Kawanabe, N., Kurosaka, H., Takano-Yamamoto, T., Yamashiro, T., 2011. The three-dimensional morphometry and cell-cell communication of the osteocyte network in chick and mouse embryonic calvaria. *Calcif. Tissue Int.* 88, 416–424.
- Sugawara, Y., Kamioka, H., Honjo, T., Tezuka, K.I., Takano-Yamamoto, T., 2005. Three-dimensional reconstruction of chick calvarial osteocytes and their cell processes using confocal microscopy. *Bone* 36, 877–883.
- Sørensen, M.S., Qvortrup, K., Friis, M., Frisch, T., Winter 2005/2006. Lacuno-canalicular pathways and barriers in perilymphatic bone. *Registry (NIDCD)* 13 (2),

- 2–5.
- Vashishth, D., Verborgt, O., Divine, G., Schaffler, M.B., Fyhrie, D.P., 2000. Decline in osteocyte lacunar density in human cortical bone is associated with accumulation of microcracks with age. *Bone* 26, 375–380.
- Zehnder, A.F., Kristiansen, A.G., Adams, J.C., Kujawa, S.G., Merchant, S.N., McKenna, M.J., 2006. Osteoprotegerin knockout mice demonstrate abnormal remodeling of the otic capsule and progressive hearing loss. *Laryngoscope* 116, 201–206.
- Zehnder, A.F., Kristiansen, A.G., Adams, J.C., Merchant, S.N., McKenna, M.J., 2005. Osteoprotegerin in the inner ear may inhibit bone remodeling in the otic capsule. *Laryngoscope* 115, 172–177.